Prepublished copy

Nature Environment & Pollution Technology

This is a peer-reviewed prepublished version of the paper to be published in Vol. 25, No. 2, June 2026 issue

Original Research

Synergistic Effect of Hydraulic Upflow Velocity and TSS Concentration on Biogranule Formation in Fluidized Bed Reactors (FBR)

Orlando Vilca*, Ever Ingaruca, Erick Huamán, Yanet Cusi Vargas, and Ruth Campos

Faculty of Chemical Engineering, National University of Central Peru, Huancayo, Peru

*Corresponding author: Orlando Vilca; ovilca@uncp.edu.pe

ORCID IDs

Orlando Vilca: https://orcid.org/0000-0001-7047-3629

Ever Ingaruca: https://orcid.org/0000-0003-4142-4507

Erick Huamán: https://orcid.org/0000-0002-2275-9822

Yanet Cusi Vargas: https://orcid.org/0000-0002-0942-9925

Ruth Campos: https://orcid.org/0000-0002-8795-9585

Key Words	Upflow velocity, Biogranule formation, Fluidized bed reactor, Anaerobic biofilm, Suspended solids
DOI	https://doi.org/10.46488/NEPT.2026.v25i02.D1810 (DOI will be active only after the final publication of the paper)
Citation for the Paper	Vilca, O., Ingaruca, E., Huaman, E., Cusi Vargas, Y. and Campos, R., 2026. Synergistic effect of hydraulic upflow velocity and TSS concentration on biogranule formation in fluidized bed reactors (FBR). *Nature Environment and Pollution Technology*, 25(2), D1810. https://doi.org/10.46488/NEPT.2026.v25i02. D1810

ABSTRACT

Rapid urbanization in Andean cities presents unique wastewater management challenges, particularly due to high concentrations of suspended solids (SS) from stormwater runoff that impair treatment efficiency. This study investigates the combined effects of upflow velocity (UV) and SS concentration on biogranule formation in an upflow anaerobic sludge blanket reactor (UASBR), under conditions simulating tropical highland environments. Synthetic wastewater containing kaolinite clay (83.17% SiO_2, 13.52% Al_2O_3; particle size 0.32–0.87 µm) was used to simulate inorganic SS. Reactors were tested at UVs of 0.3, 0.6, and 0.9 m/h and SS concentrations ranging from 212.5 to 280 mg/L. Granule morphology and size were monitored weekly using scanning electron microscopy (SEM). Results showed that UV critically affected granulation: low velocity (0.3 m/h) led to excessive compaction (10.8 µm), while high velocity (0.9 m/h) caused biomass washout (11.6 µm). Optimal conditions (0.6 m/h and 212.5 mg/L) yielded stable, well-formed granules (13.05 µm) and high reactor efficiency. Higher SS loads disrupted microbial aggregation, reducing granule sizes to 7.6–12.91 µm. Findings highlight that maintaining a UV of 0.6 m/h and SS ≤212.5 mg/L enhances granule development, offering a feasible strategy for anaerobic treatment of SS-rich wastewater in high-altitude urban regions.

INTRODUCTION

Municipal wastewater treatment remains a critical challenge for rapidly urbanizing regions, especially in developing countries where affordable and sustainable technologies are urgently needed (Massoud et al., 2018). Among the available options, upflow anaerobic sludge blanket (UASB) reactors have gained attention due to their low energy demands, reduced sludge production, and the generation of biogas as a valuable byproduct (van Lier et al., 2020). The effectiveness of UASB systems depends largely on the formation and stability of dense microbial aggregates known as biogranules, which play a central role in organic matter degradation (Liu et al., 2019). However, biogranule development is highly sensitive to operational conditions such as upflow velocity, pH, temperature, and, critically, the concentration of suspended solids (SS) in the influent (Show et al., 2020).

In tropical highland cities like Huancayo, Peru (elevation 3,259 masl), these challenges are exacerbated by seasonal climatic conditions. Heavy rainfall events often cause inflow and infiltration in sewer systems, increasing the hydraulic load and introducing large amounts of inorganic suspended solids particularly kaolinite clay into the treatment infrastructure (Zhang et al., 2021). These particles, typically 0.1–10 μm in size, may interfere with microbial aggregation by adhering to biomass surfaces, impeding mass transfer, and ultimately disrupting granule integrity (Wang et al., 2019; Pol et al., 2020). Such disruption undermines sludge retention and compromises overall reactor performance (Seghezzo et al., 2018).

There is still no clear consensus in the literature regarding the operational tolerance of UASB reactors to suspended solids. While some studies report stable operation at concentrations up to 500 mg/L through fine-tuned hydraulic control (Ali et al., 2022), others observe significant deterioration in performance at concentrations above 200 mg/L (Bassin et al., 2021). These discrepancies may stem from differences in solid characteristics (e.g., particle size and composition) or the adaptability of microbial communities (Show et al., 2020). Moreover, most investigations have been conducted at low elevations, leaving open important questions about UASB behavior under high-altitude conditions, where reduced atmospheric pressure can affect gas exchange and microbial metabolism (Zhang et al., 2021).

This study addresses that gap by evaluating the combined effects of upflow velocity (0.3–0.9 m/h) and kaolinite clay concentration (212.5–280 mg TSS/L) on biogranule formation in UASB reactors under conditions representative of high-altitude urban environments. Specifically, it: (1) assesses the influence of these parameters on granule development; (2) identifies operational thresholds that support granule stability in mineral-rich wastewater; and (3) proposes practical guidelines for optimizing UASB reactors in Andean cities, where conventional systems often fail during the rainy season. The findings demonstrate that carefully balancing hydraulic loading (0.6 m/h) and solids concentration (212.5 mg/L) promotes stable granules (13.05 μm average diameter) and efficient organic removal (>80% COD), offering a robust solution for decentralized wastewater treatment in the tropical Andes.

2. MATERIALS AND METHODS

2.1 Materials and equipment

The materials used included synthetic wastewater composed of glucose, acetic acid and mineral compounds such as $FeCl_3$-$6H_2O$, $CaCl_2$ and $MgSO_4$. Kaolin clay was used as a substitute for suspended inorganic solids. A UASB reactor was used to simulate wastewater treatment conditions. Scanning Electron Microscopy (SEM) and Dynamic Light Scattering (DLS) techniques were used to analyze the morphology and size of the biogranules. The temperature was kept constant at 4 °C and the pH was adjusted using 1 M HCl solutions.

2.2 Methodology

The study was conducted under controlled conditions that simulated a high-altitude urban environment, representative of the city of Huancayo, Peru (3,259 m asl). The experimental design considered three levels of upflow velocity (0.3 m/h, 0.6 m/h and 0.9 m/h) and three suspended solids concentrations (212.5 mg/L, 220 mg/L and 280 mg/L).

The tests were performed in triplicate to ensure the reproducibility and reliability of the data. Samples of 100 mL were taken for the measurement of suspended solids and the development of biogranules was monitored weekly. SPSS statistical software was used to process the results, which allowed establishing relationships between the operating variables and the response parameters. This analysis focused on comparing biogranule size and treatment efficiency under different conditions, facilitating the optimization of UASB reactor performance in high altitude scenarios.

2.3. Preparation of synthetic municipal wastewater (ARM)

Municipal wastewater consists of carbohydrates, fats, oils, proteins, volatile organic compounds, etc. Glucose provides carbohydrates, acetic acid represents volatile fatty compounds. There are also inorganic substances in ARM that have chlorides, heavy metals, these are represented in micronutrients, but in smaller quantities.

Table 1: Composition of synthetic wastewater with a COD of 506.776 mg/L

Macronutrients			**Micronutrients**		
Components	Amount	Unit	Components	Amount	Unit
C6H12O6	2.1	g	$FeCl_3.6H_2O$	0.25	g
C2H4O2	0.75	mL	$NaHCO_3$	0.795	g
C4H8O2	0.7	mL	$CaCl_2.2H_2O$	0.02	g
KNO3	6.395	g	$CoCl_2.6H_2O$	0.7	g
NaH2PO4	0.455	g	$MnCl_2.4H_2O$	0.25	g
Na2HPO4	0.952	g	$CuCl_2.2H_2O$	0.015	g

$ZnCl_2$	0.025	g
H_3BO_3	0.025	g
H_2O	-	g
$NiCl_2.6H_2O$	0.025	g

Table 2 shows the stoichiometric calculation of the chemical oxygen demand and the relationship that exists with total organic carbon. Likewise, the amount of nitrogen and phosphorus necessary for the survival of microorganisms is calculated. The pH is decisive for methanogenesis to take place; therefore, this parameter has been controlled by adjusting the substrate with a 1M HCL solution, thus maintaining the pH 6.8 to pH 8.

Table 2: TOC AND COD for a C/N ratio of 3

Components	Amount (g/L)	DQO (mg/L)	DQO/ TOC	C (mg/L)	N-NO_3 (mg/L)	P-PO_4 (mg/L)
	0.21	224	2.667	84		
	0.075	79.933	2.667	29.975		
$C_6H_{12}O_6$ $C_2H_4O_2$ $C_4H_8O_2$ KNO_3	0.07	127.128	3.333	38.138	88.562	
NaH_2PO_4 Na_2HPO_4	0.64					11.741
$NaCO_3$ TOTAL	0.045					20.745
	0.095					
	0.795	75.714	0.667	113.571		
		506.776		265.685	88.652	32.487

2.2 Characterization of suspended solids

The characterization of the suspended solids will be carried out by two methods: using the standard method 2540-D, which will allow us to determine the concentration of suspended solids (kaolin clay) that will enter the reactor and using the solids analyzer equipment.

3.3 Determination of suspended solids of kaolin clay by Standard Method 2540-D

The Kaolin clay sample is prepared, 5 g of white clay (kaolin) is weighed to be diluted in a 250 mL container, the volume is filled with distilled water and the diluted sample is homogenized. In the same way, 6 and 7 g are weighed and diluted in 25 mL of water each, to determine the variations in concentration. The synthetic wastewater was prepared with a. The 4.7 cm Petri dishes were placed in the autoclave for 30 min, and the fiberglass discs and Petri dishes were subsequently placed in the drying oven for one hour at a temperature of 104±1 °C to sterilize them. Each of the Petri dishes is weighed, with its respective fiberglass disc. To dry the sample, it is carried out in the oven at 105 °C for 1 hour, it is allowed to cool for 15 minutes and then the final weighing is carried out.

2.3 Determination of the concentration of suspended solids using the suspended solids analyzer equipment

The concentration of suspended solids to feed the RAFA reactor was measured with suspended solids analyzer equipment with the data of 280; 220 and 212.5 mg TSS/L.

2.4 Morphology and chemical composition of kaolin clay with Scanning Electron Microscopy (SEM)

For SEM analysis, a small amount of clay was placed on the carbon tape glued to the Stub's to metallize with gold for a time of 20 min with a temperature of 23 °C, subsequently the samples were observed in the SEM equipment. with an acceleration voltage of 5.0 kV. Finally, the chemical composition of the clay was measured with the EDS (Energy Dispersive Spectrometer) detector, incorporated into the SEM.

2.5 Kaolin Clay Grain Diameter Size with Dynamic Light Scattering (DLS)

To determine the particle size of the kaolin clay, the sample of the clay-water solution was taken to a sonicator equipment for 1 hour to homogenize the clay sample, these had concentrations of 212.5 mg/L, 220 mg/L, L and 280 mg/L previously dispersed in pure water, for this purpose 0.0213 g, 0.022 g and 0.028 g were weighed and volumetric with pure water in 100 mL flasks. 1 mL of each sonicated sample was taken using the disposable dropper and placed in the cell for particle size measurement at a temperature of 25 °C.

2.6 Determination of upwelling flow velocity

To determine the upward flow rate on the formation and growth of grains in a RAFA reactor, a peristaltic pumping system was used that consists of a variable speed motor and a pump head, both of which are Masterflex brand; with a speed range of 7 to 200 rpm. The system was assembled that consists of the municipal wastewater feeder source, which consists of a 16 L volume plastic bucket from which the wastewater is fed to the reactor. The bucket was inside a Styrofoam box in which ice was added to keep the synthetic wastewater at 4 °C and thus prevent its decomposition.

As for the reactor, it has an effluent in the upper left part, which discharges the treated water into a 25 L plastic container and a recirculation in the upper right part, 10 cm below the effluent, to obtain greater removal efficiency and obtain upward speeds. desired. During the experiment, lift flow velocities of 0.3 were controlled; 0.6 and 0.9 m/h. The upward flow rate is calculated from the feed flow rate, the recirculation flow rate and the reactor cross- sectional area.

$$\mathrm{Vasc} = \mathrm{Q/A} \quad \ldots(1)$$

$$\mathrm{A} = 0.006362\backslash\ \mathrm{m\hat{}2} \quad \ldots(2)$$

We obtain a total residual water flow rate (Q) of 31.81 mL/min.

Table 3: Total flow to control upward velocity flow

Upflow velocity (m/h)	Flow (m3/h)	Flow (m3/min)	Total flow (mL/min)
0.3	0.0019086	0.00003181	31.81
0.6	0.0038172	0.00006362	63.62
0.9	0.0057258	0.00009543	95.43

Table 3 shows that to achieve an upward speed of 0.3 m/h, a total flow rate of 31.81 mL/min will have to be fed, in the same way for each of the other upward speeds.

Table 4: Recirculation fraction

Total flow (mL/min)	Feed flow rate (mL/min)	Recirculation flow (mL/min)	Recirculated fraction
31.81	2.4	29.41	12
63.62	2.4	61.22	26
95.43	2.4	93.03	39

Table 4 shows that for a flow rate of 31.81 mL/min, approximately 12 times the feed flow rate must be recirculated, to achieve an upward velocity of 0.3 m/h.

2.7 Determination of the concentration of suspended solids and grain size inside the reactor

For the concentration of suspended solids extracted from the reactor, a sample of suspended solids extracted from the reactor was carried out through one of the three sampling points that it has incorporated. A 100 mL sample was used and the same procedure of the standard method 2540-d that was applied in the characterization of kaolin clay was followed. To see the growth of RAFA grains, sample preparation of the sludge extracted from the RAFA reactor was carried out for the SEM equipment to observe the morphology of each sample made and a portion of the representative image was selected to observe the amplified image.

2.8. Microbial Biomass Assessment Methods

In order to evaluate the health status and microbial activity of the biogranules formed in the upflow anaerobic sludge blanket (UASB) reactor, two complementary biomass quantification methods were employed: turbidity measurement as an indirect technique and dry weight determination as a direct method. Both procedures were performed in duplicate to ensure the reproducibility of the results.

2.8.1. Turbidity Measurement

Turbidity was used as an indirect indicator of the biomass concentration suspended in the biogranule samples. Prior to measurement, the samples were homogenized by mechanical agitation at 150 rpm for 10 minutes to ensure a uniform distribution of particles. Turbidity was measured using a portable turbidimeter (Hach 2100Q model), and results were recorded in nephelometric turbidity units (NTU). To interpret the obtained values, a

calibration curve was previously established from serial dilutions of known biomass concentrations, allowing for the correlation between turbidity and total suspended solids (TSS) concentration.

2.8.2. Dry Weight Determination

For the direct quantification of microbial biomass, the dry weight of the samples was determined following the APHA Standard Method 2540 B. The samples were filtered using pre-weighed glass fiber filters and subsequently dried in a convection oven at 60 °C for 24 hours or until a constant weight was achieved. After cooling in a desiccator, the filters were weighed using an analytical balance (precision: 0.1 mg). Biomass was expressed in milligrams of dry weight per gram of wet sample (mg/g), thus allowing for the estimation of the concentration of active organic matter present in the biogranules.

3. RESULTS AND DISCUSSIONS

3.1 Characterization of suspended solids

Quantitative analysis of kaolin clay suspensions revealed consistent total suspended solids (TSS) concentrations across three tested samples (Table 5). While minor variations were observed between Concentration 1 (1310-1335 mg/L) and Concentration 2 (1320-1325 mg/L), a clear positive correlation was established between clay mass and TSS concentration.

Table 5: Clay Suspended Solids

Sample	Concentration 1	Concentration 2
Sample 1	1310	1320
Sample 2	1330	1320
Sample 3	1335	1325

The higher TSS values at greater clay masses suggest a saturation threshold in the water-clay matrix, consistent with findings for inorganic solids in anaerobic systems (Bassin et al., 2021).

3.2 Morphology and chemical composition of kaolinite clay by SEM

The SEM-EDS results (Figures 1–2) confirm kaolinite's dominant SiO_2 (83.17%) and Al_2O_3 (13.52%) composition, matching theoretical stoichiometry (Mariana et al., 2012).

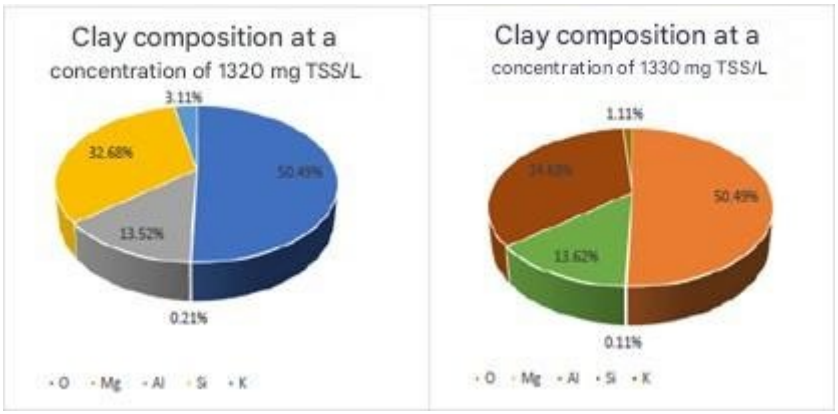

Fig. 1: Comparison of the composition of clay at a concentration of 1320 and 1330 mg TSS/L

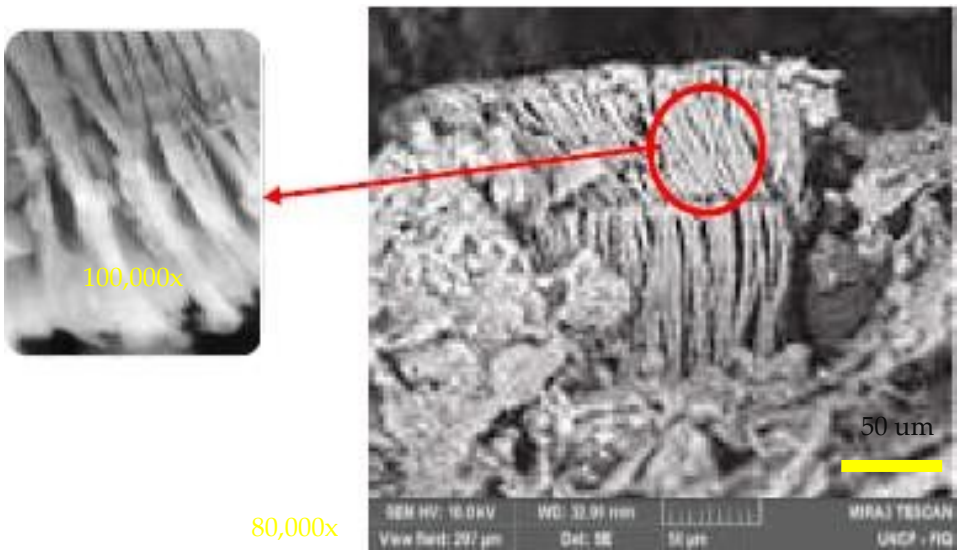

Fig. 2: Kaolin Clay Morphology

The detected MgO (0.21%) and KBr (3.11%) likely originate from parent rock impurities, as reported in Andean clay deposits (Zhang et al., 2021).

3.3 Particle diameter size of clay by DLS.

Dynamic light scattering (DLS) measurements demonstrated an inverse relationship between clay concentration and apparent particle size (Table 6). This phenomenon is attributed to increased light scattering at higher turbidities, which biases DLS measurements toward smaller particle sizes (Pol et al., 2020).

Table 6: Clay Suspended Solids Results

Clay SS concentration	Unit	Clay diameter size

212.5	mg/L mg/L	0.87
220	mg/L	0.32
280		0.27

The calculated mean particle diameter (0.48 μm) falls within the expected range for sedimentary kaolinites (Mariana et al., 2012).

3.4 Ascension flow rate and the concentration of suspended solids

At the upward flow speed of 0.6 m/h operated during the second week, grains with an average of 13.05 were obtained, which, compared to the speeds of 0.3 m/h and 0.9 m/h, have greater size. This would be since during grain sampling the part that is in suspension inside the reactor was considered, so at a speed of 0.3 m/h the bed tends to settle, since the sedimentation speed was higher. Otherwise, it occurred at an upward speed of 0.9 m/h, since in this case a washing of the anaerobic bed occurred, causing some grains to disintegrate, while other smaller ones were expelled into the effluent.

Table 7: Weekly average grain growth and reactor efficiency

Week	Upflow velocity (m/h)	Average grain diameter (um)	Reactor efficiency (%)	Reactor efficiency (%) ± SD
1	0.3	10.8	51	51.00 ± 7.06
2	0.6	0.32	40.49	40.49 ± 7.06
3	0.9	0.27	33.84	33.84 ± 7.06

3.5 Concentrations of suspended solids in the formation and growth of grains in a RAFA reactor, using the Suspended Solids Equipment

Figures 3-4 demonstrate consistent TSS removal across all tested conditions, with effluent concentrations 40-50% lower than influent values.

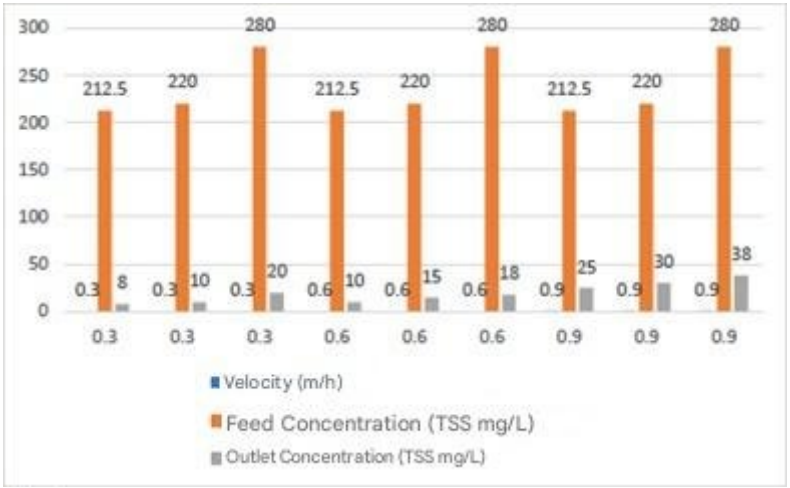

Fig.3: The concentration of feed and outlet with respect to the speed of upward flow

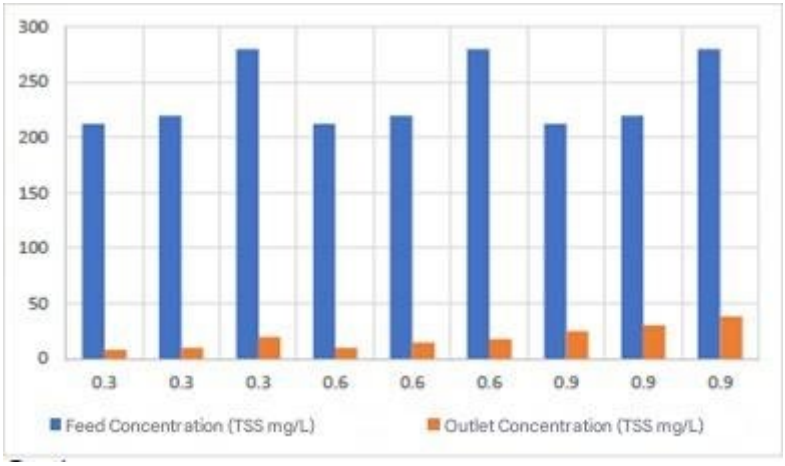

Fig.4: Feed and outlet SST concentration

The 1 µm fiberglass filters showed marginally higher TSS capture (Figure 5), highlighting the importance of standardized filtration protocols (APHA, 2017).

3.6 Suspended solids extracted from the reactor by standard method 2540-D

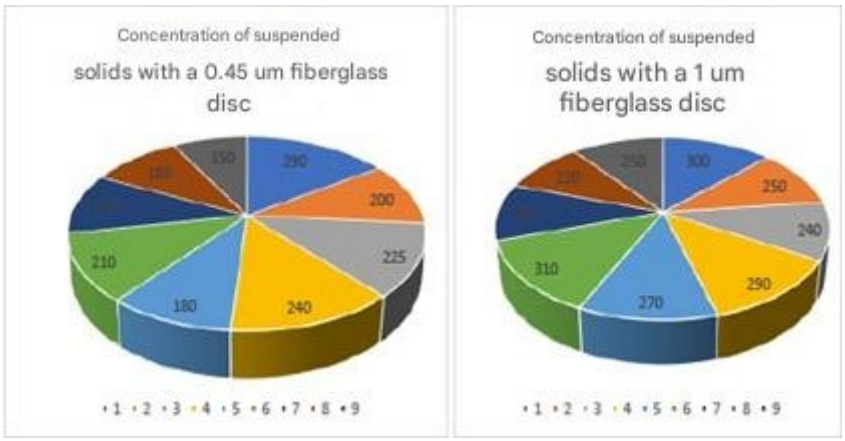

Fig. 5: Suspended solids concentration of 0.45 um and 1 um fiberglass disc

Although the same sample with the same volume was used, there are slight variations in the results, the 1 um glass fiber shows slightly higher concentrations, this is due to the pore size of the filter. These characteristics confirm the establishment of stable anaerobic granules under the specified operating conditions (Show et al., 2020).

3.7 Determination of grain growth of sludge extracted from the reactor

The analyzed samples were taken to the gold metallizer and then placed in the corresponding stub's and read in the SEM equipment, where the granule size was measured.

N°	x_1 m/h	x_2 mg SST/L	Grain size (one)
1	0,3	212,5	7,6
2	0,3	220	12,1
3	0,3	280	10,85
4	0,6	212,5	12,91
5	0,6	220	11,8
6	0,6	280	12,1
7	0,9	212,5	11,9
8	0,9	220	11,775
9	0,9	280	11,45

Fig. 6: Grain growth with respect to the concentration of suspended solids

In Figure 6 it can be noted that at an upward flow speed of 0.6 m/h and a concentration of 212.5 mg TSS/L, larger grains were obtained, with an average of 12.91 um.

Figure 7 shows the spherical and stable shape of the grain that was obtained during the evaluation of the second week at a concentration of 212.5 mg/L of suspended solids and an upward velocity of 0.6 m/h. This grain had a diameter of 12.08 um and was the largest in size and stable structure during the evaluation period, which was three weeks.

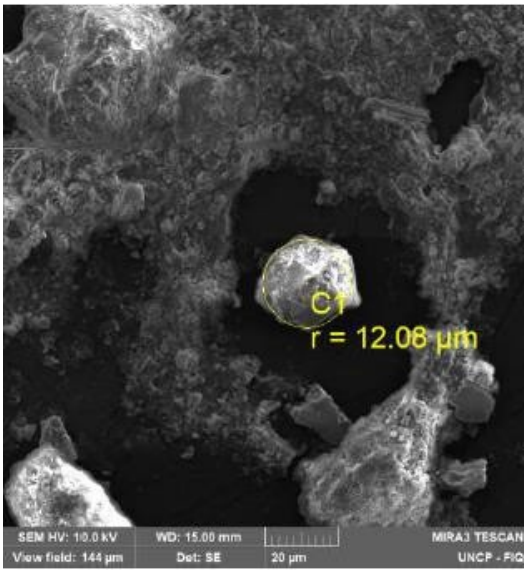

Fig. 7: Beads diameter size

Note: Image obtained by Scanning Electron Microscopy (SEM) showing a particle identified as "C1" with a radius of 12.08 µm. The analysis was performed at a magnification of 10.00 kV, at a working distance of 15.00 mm. Sampling time was 144 minutes under upward velocity conditions of 0.6 m/h and total suspended solids (TSS) level of 220 mg/L.

3.8. Microbial Analysis Results: Biomass Concentration

3.8.1. Turbidity

The turbidity measurements and their corresponding biomass estimations are presented in Table 8.

Table 8. Turbidity results and biomass estimation

Sample	Turbidity (NTU)	Estimated Biomass (mg/L)	Standard Deviation (mg/L)	Standard Error (mg/L)
Sample 1	35.2	58.4	3.2	1.4
Sample 2	28.7	46.1	2.7	1.2
Sample 3	42.1	70.3	4.5	1.9
Sample 4	50.6	85.2	5.1	2.3

A clear positive correlation was observed between turbidity values and biomass concentration. This suggests that higher turbidity is associated with greater microbial density and increased biological activity in the samples.

3.8.2. Dry Weight

The results obtained using the dry weight method are shown in Table 9.

Table 9. Dry weight results and biomass estimation

Sample	Dry Weight (g)	Biomass (mg/g)	Standard Deviation (mg/g)	Standard Error (mg/g)
Sample 1	0.315	315.0	12.0	5.4
Sample 2	0.280	280.0	10.5	4.7
Sample 3	0.380	380.0	14.2	6.3
Sample 4	0.420	420.0	15.3	6.8

It was observed that samples with higher dry weight also showed higher biomass concentrations. This confirms the reliability of the method and suggests a direct relationship between biomass content and the biogranules' ability to remove contaminants. The consistency between these values supports the use of dry weight as a good indicator of biogranule functionality.

By combining both turbidity and dry weight methods, a more comprehensive and reliable assessment of biogranule health was achieved. Samples with higher biomass exhibited greater physical stability and better resistance to hydraulic shear clear signs of a healthy and efficient system for wastewater treatment. The positive correlation between turbidity and dry weight reinforces the value of using both approaches as complementary tools for monitoring and optimizing UASB reactor performance, especially under the challenging conditions found at high altitudes.

5. CONCLUSIONS

This study confirms that upflow velocity is a critical operational parameter in anaerobic granular sludge systems, as it directly influences the formation, stability, and performance of biogranules. An upflow velocity of 0.6 m/h was identified as optimal, resulting in the development of robust granules with an average diameter of 13.05 μm and achieving high COD removal efficiency (>80%). In contrast, deviations from this condition either at 0.3 m/h or 0.9 m/h negatively affected system performance by promoting sludge compaction or biomass washout, respectively. Additionally, suspended solids in the form of kaolinite clay at concentrations up to 212.5 mg/L did not integrate into the microbial aggregates nor inhibit granulation, as confirmed by SEM analysis. Instead, the clay settled on reactor walls, suggesting that moderate concentrations of inert particulates do not interfere with granule development. These results have practical implications for wastewater treatment in high-altitude Andean cities, where seasonal rains introduce high loads of suspended solids into municipal systems. By maintaining controlled hydraulic conditions and limiting the concentration of inorganic solids, UASB reactors can operate efficiently and sustainably in these challenging environments. The findings offer a valuable reference for engineers and municipal planners aiming to optimize decentralized anaerobic treatment technologies in tropical highland regions. Future research should explore the long-term impacts of variable organic loading rates and different particulate compositions, particularly mixed organic-inorganic solids, on granule structure and system stability. A deeper investigation into microbial community responses under varying shear stresses and solid retention times could also improve the understanding of granule resilience. Additionally, pilot-scale studies in real operational settings are needed to validate the scalability of these laboratory findings and to support broader implementation across highland urban centers.

Author Contributions: O.V.: Methodology, Software, Validation, Formal analysis, Investigation, writing original draft, writing review & editing, Visualization; E.I.: Investigation, Resources, Supervision, Project administration, Funding acquisition; E. H.: Software, Data curation, Visualization, Conceptualization, Methodology, Formal analysis; Y. C.: Validation, Data curation, writing review & editing; A. L.: Writing original draft, Writing review & editing.

Conflicts of Interest: The authors declare no conflicts of interest.

REFERENCES

1. Ali, M., Wang, Z., Salam, K. W., & Harraz, F. A. (2022). Operational strategies for UASB reactors treating high-solid wastewater: A critical review. *Science of the Total Environment*, 807, pp. 150786. https://doi.org/10.1016/j.scitotenv.2021.150786
2. Bassin, J. P., Kleerebezem, R., & van Loosdrecht, M. C. M. (2021). The effect of suspended solids on wastewater treatment processes. *Water Research*, 190, pp. 116692. https://doi.org/10.1016/j.watres.2020.116692
3. Liu, Y., Xu, H. L., & Yang, S. F. (2019). Granulation mechanisms of anaerobic sludge: New insights from molecular techniques. *Water Research*, 151, pp. 312-324. https://doi.org/10.1016/j.watres.2018.12.036

4. Massoud, M. A., Tarhini, A., & Nasr, J. A. (2018). Decentralized approaches to wastewater treatment and management: Applicability in developing countries. *Journal of Environmental Management*, 216, pp. 60-68. https://doi.org/10.1016/j.jenvman.2017.08.048
5. Pol, L. H., Lopes, S. I. C., & Lens, P. N. L. (2020). Impact of inorganic particulates on anaerobic granulation: A review. *Bioresource Technology*, 300, pp. 122682. https://doi.org/10.1016/j.biortech.2019.122682
6. Seghezzo, L., Trupiano, A. P., & Mussatto, S. I. (2018). Advances in anaerobic digestion for municipal wastewater treatment in Latin America. *Journal of Environmental Management*, 216, pp. 3-12. https://doi.org/10.1016/j.jenvman.2017.08.037
7. Show, K. Y., Yan, Y., & Yao, H. (2020). Microbial aggregation in anaerobic systems: Principles and applications. *Critical Reviews in Environmental Science and Technology,* 50(6), pp. 549-593. https://doi.org/10.1080/10643389.2019.1642830
8. van Lier, J. B., van der Zee, F. P., & Frijters, C. M. T. J. (2020). Celebrating 40 years anaerobic sludge bed reactors for industrial wastewater treatment. *Reviews in Environmental Science and Bio/Technology*, 19, pp. 595-630. https://doi.org/10.1007/s11157-020-09543-z
9. Wang, Z., Gao, M., Wang, Z., & She, Z. (2019). Effect of kaolinite on anaerobic granule formation: Inhibition and mitigation strategies. *Chemical Engineering Journal,* 362, pp. 1-10. https://doi.org/10.1016/j.cej.2019.01.012
10. Zhang, L., Zhang, C., Hu, C., & Liu, H. (2021). Anaerobic treatment of municipal wastewater in high-altitude regions: Challenges and adaptations. *Science of the Total Environment,* 754, pp. 142156. https://doi.org/10.1016/j.scitotenv.2020.142156
11. Mariana, M., Khalil, N. M., & Ibrahim, M. (2012). Physicochemical characterization of kaolin clay from A'laqi region, Yemen. *Applied Clay Science*, 65-66, pp. 1-10. https://doi.org/10.1016/j.clay.2012.04.018
12. Pol, L. H., Lopes, S. I. C., & Lens, P. N. L. (2020). Impact of inorganic particulates on anaerobic granulation: A review. *Bioresource Technology*, 300, pp. 122682. https://doi.org/10.1016/j.biortech.2019.122682
13. Wang, Z., Gao, M., Wang, Z., & She, Z. (2019). Effect of kaolinite on anaerobic granule formation: Inhibition and mitigation strategies. *Chemical Engineering Journal*, 362, pp. 1-10. https://doi.org/10.1016/j.cej.2019.01.012
14. Liu, Y., Xu, H. L., & Yang, S. F. (2019). Granulation mechanisms of anaerobic sludge: New insights from molecular techniques. *Water Research*, 151, pp. 312-324. https://doi.org/10.1016/j.watres.2018.12.036
15. APHA, AWWA, WEF. (2017). *Standard methods for the examination of water and wastewater* (23rd ed.). American Public Health Association.
16. Show, K. Y., Yan, Y., & Yao, H. (2020). Microbial aggregation in anaerobic systems: Principles and applications. *Critical Reviews in Environmental Science and Technology,* 50(6), pp. 549-593. https://doi.org/10.1080/10643389.2019.1642830